

Implementation of Velocity Profiles in Group Control of Elevator Systems

Zavarin Gagov, Young Cheol Cho, Wook Hyun Kwon

*Control Information Systems Lab., School of Electrical Engineering,
Seoul National University, Seoul, 151-742, Korea*

Key Words : velocity profile, velocity area, group controller

ABSTRACT

In this paper, we present new calculation procedure to generate reference velocity profiles for elevator systems. Our aim is to simplify existent calculation methods by avoiding repetitive derivations of similar results. In addition, we focus our attention on so called stop control point in velocity profile, demonstrating its impact over global system performance in terms of group control. We support our derivations by implementation algorithm and examples.

1. INTRODUCTION

Dealing with the motion of the elevator, either dynamical or kinematics approaches are reasonable in different situations. From classical control point of view, in order to achieve desired features realistically, applied forces and torques should be considered. On the other hand, in multiple elevator systems, so called *group controller* (GC) relies on already applied conventional control to each car. The objective of GC is to provide best global performance, dispatching all available elevator cars in response to multiple passenger demands. In order to find an optimal solution of such control problem, it is necessary to estimate all possible solutions related with timing characteristics. In this context, we believe that the knowledge of car kinematics is a meaningful and important factor in enhancing the global performance of elevator group control systems.

More than in papers, commonly the information concerning optimal car kinematics is published in patents. In this regard, good reference is (Williams et al 1985), where optimal velocity generation and implementation are discussed extensively. In the field of elevator systems, the book of Barney and Dos Santos (Barney and Dos Santos 1985), contains brief notes about speed profiles. The concept of profile generation segmenting, and its implementation in elevator systems was first suggested by Molz. One of his recently updated results is given in (Molz 1991). Another researcher, Peters (Peters 1995), concentrated on enhancing and correcting some of the results published by Molz. In 2000, we presented work (Gagov et al 2000) with accent on the relation between car kinematics and the parameters of GC. In 1998, there appeared paper (Beldiman et al 1998), where so called trajectory of high rise buildings was explored either as an optimal control problem, and as an object of heuristic search. Also, velocity profiles were used to estimate global evacuation time during emergency (Klote 1993).

In this paper, we present optimized version of the calculations presented in (Molz 1991) and

(Peters 1995). Obtaining comparable results of car kinematics, we avoid multiple integration and repetitive calculations. In addition, we suggest short implementation algorithm for generation of velocity table and velocity profiles. Finally, we focus our attention on the location of so called *stop control points*, demonstrating their importance in car dispatching by examples.

In Section 2 we explain the framework of velocity profile calculations. In Section 3 we derive the velocity parameters using solutions of differential equations. In Section 4, small implementation algorithm is presented. In Section 5, we use particular examples to demonstrate the algorithm and to discuss nonlinear behavior of some parameters of elevator system. Finally, we finish with concluding remarks.

2. FRAMEWORK OF VELOCITY PROFILES GENERATION

2.2 Logic and Symmetry in Velocity Profile

As we pointed out in the introduction, GC is *not* directly involved in the conventional control. For the purpose of optimal car dispatching, GC deals with selected *discrete states* and with the time points relative to them.

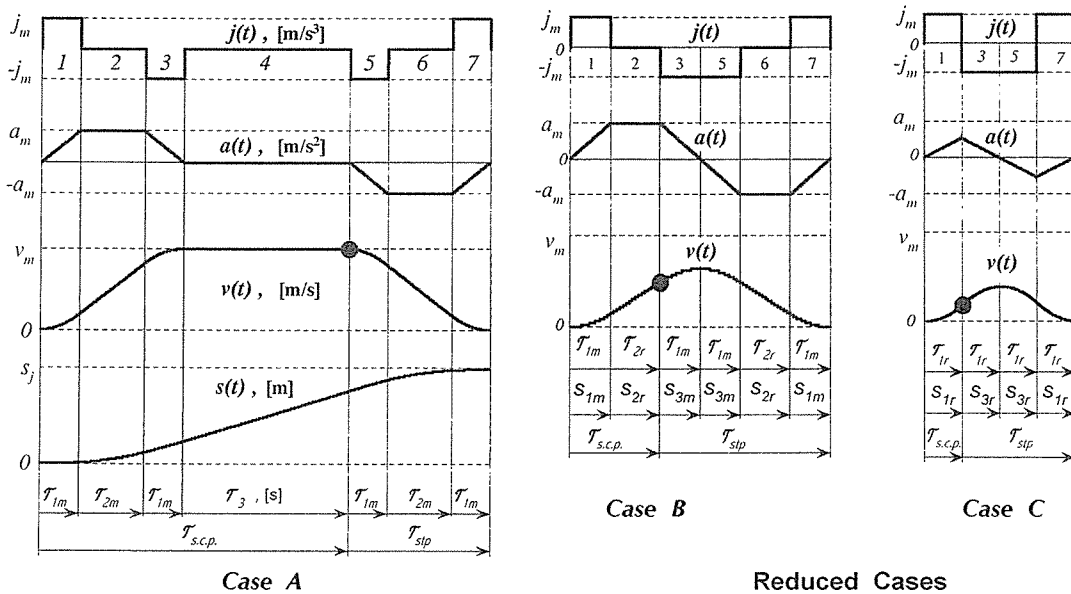


Figure 1, Three cases of velocity profiles generation:

A: Max acceleration and max velocity are reached

B: Max acceleration is reached, but max velocity is not.

C: Neither max acceleration, nor max velocity are reached.

In Fig.1, (case A) the relations between the *jerk* ($j, [m/s^3]$), the *acceleration*, ($a, [m/s^2]$), the *velocity* ($v, [m/s]$), and the *displacement* ($s, [m]$) of elevator car are shown. The four variables in Fig.1, (case A) are mathematically related by subsequent integration from top to bottom with respect to the time. Conversely, they are related with respective derivations from bottom to top with respect to the time. There are seven clearly distinguishable *velocity areas*, we enumerated them by digits 1,2,...,7. Encountered areas can be grouped behaviorally as follows: The characteristic of *areas 1,3,5,7* is their constant maximal jerk, the *areas 2,6* are characterized with constant maximal acceleration, and in *area 4* there is constant maximal (contract) velocity. Also, it is important that the switching from one area to another is governed by abrupt changes of the jerk. Our objective is to solve constrained problem,

looking for minimal journey time τ_j as a function of journey distance s_j , and subject to three limitations: allowed maximal jerk $\pm j_m$, allowed maximal acceleration $\pm a_m$, and maximal possible velocity v_m .

$$\tau_j = \min f(s_j, j, a, v), \text{ where} \quad (1)$$

$$|j| \leq j_m, |a| \leq a_m, v \leq v_m$$

The constraint $v < v_m$ is technical, due to the limitations of the motor abilities, or due to safety reasons in some cases. The constraints $|j| \leq j_m$ and $|a| \leq a_m$ mostly follow the requirements of passenger's comfort.

It is important to observe the logic of the appearance of all different areas and the existent symmetry of the velocity curve in Fig.1, (*case A*). Following the constant jerk in *areas 1,3,5,7*, the time duration needed either for reaching v_m or for decreasing the acceleration to zero is equal. Respectively, time slices relevant to *areas 1,3,5,7* are denoted by the equal duration τ_1 . Hence, any possible change in the curve parameters have to preserve mentioned slices being equal to the same τ_{1r} or τ_{1m} . In the whole paper, indexing “*m*” stands for maximal value, and indexing “*r*” indicates that given value is *reduced* and guaranteed to be smaller than the maximal possible. Further, due to the constant maximal acceleration in *areas 2,6*, their time slices, denoted by τ_2 , (τ_{2r}, τ_{2m}) are with equal duration too.

In Fig.1, (*case B, case C*), two reduced situation of the car trip are shown. Their enumeration corresponds to the area enumeration in *case A*. Due to the limited time (or limited travelling distance), in *case B* maximal acceleration is reached, but the maximal speed is not. In *case C*, neither the velocity, nor the acceleration succeed to reach their maximal values.

Following the desire of achieving fastest possible journey of the car, initially parameters are designed to guarantee certain sequence. For example, achieving of maximal velocity v_m is possible only if maximal acceleration has been reached already. As well as, movement with constant velocity is allowed only if maximal velocity v_m has been previously reached. Following the preservation of case subsequence, in any *case A, B* or *C*, only *one kind* (group) of equally long time slices is allowed to change simultaneously. We refer to such timing slices as a *tuning time slices*. In *case A*, the tuning time slice with duration τ_3 appears in *area 4*. We are not using annotation τ_{3r} , because there is no maximal value of τ_{3m} . In *case B*, the tuning time slices with lengths τ_{2r} appear in *areas 2* and *6*. And in *case C*, the tuning time slices with lengths τ_{1r} appear in *areas 1,3,5,7*. Following described dependencies, the accelerating and the decelerating parts of velocity profile cannot be constructed independently from each other. In order to choose appropriate decreasing part of the curve, the accelerating part have to be known. Conversely, in order to generate correct accelerating part, the decelerating part of the curve, have to be constructed in advance. In most cases, the assumption of symmetry corresponds to the reality.

2.3 The Stop Control Point

The stop control point (**s.c.p.**) has significant importance while applying kinematics parameters in GC. If we suppose that the GC suddenly decides to shorten the trip of given car, the **s.c.p.** is *the last time instant* when the decision whether to stop is allowed. The **s.c.p.** can be defined in terms of distance as well. This is *the most distant point after departure*, where

decision whether to stop or not is allowed. We can express the journey time (or displacement) as a sum time (or displacement) from departure point to **s.c.p.**, plus respective time (displacement) from **s.c.p.** to the landing point:

$$\begin{aligned}\tau_j &= \tau_{s.c.p.} + \tau_{stp} \\ s_j &= s_{s.c.p.} + s_{spt}\end{aligned}\quad (2)$$

The duration τ_{stp} stands for stopping time after **s.c.p.** and s_{spt} stands for stopping distance after **s.c.p.** In all cases (*A, B, C*), while the car is moving, the **s.c.p.** appears at the end of first appeared tuning slice. In other words, that is the moment, when the duration of given tuning slice or slices is chosen. In cases *B* and *C*, the (equal) tuning time slices are more than one, while in case *A* only τ_3 is used for tuning. In Fig.1, the stop decision points are shown by distinguishable dots on the velocity curves. Respectively:

$$\begin{aligned}\tau_{s.c.p.,A} &= 2\tau_{1m.} + \tau_{2m.} + \tau_3 & \tau_{stp,A} &= 2\tau_{1m.} + \tau_{2m.} \\ \tau_{s.c.p.,B} &= \tau_{1m.} + \tau_{2r.} & \tau_{stp,B} &= 3\tau_{1m.} + \tau_{2r.} \\ \tau_{s.c.p.,C} &= \tau_{1r.} & \tau_{stp,C} &= 3\tau_{1r.}\end{aligned}\quad (3)$$

In many cases, it is natural to assume that minimal journey time (2) is the only solution of optimality problem. However, we point out that short trip time does not necessarily comply with the optimality problem in terms of group control. The operands defined in eqns (3) and used in the sums (2), are switched from case to case by *logical conditions*. Hence, their behavior is not guaranteed to be smooth along the velocity curve. Respectively, the location of **s.c.p.** affects global performance not in terms of minimal journey time, but after implementation in group controller. Simply, the **s.c.p.** dictates the ability or not to accept given hall call at any time instant. Hence, this problem concerns heavy traffic situations. In Section 5 we demonstrate the jumping nature of **s.c.p.** by examples.

3. DERIVATION OF VELOCITY EQUATIONS

The purpose of this chapter is to give explicit kinematics dependencies looking for minimal journey time of the elevator car. Obtained final results for **s.c.b.** and the minimal journey time are needed to fill look up table for further use in elevator group control. We begin with the differential equations describing the relations between $j(t)$, $a(t)$, $v(t)$, and $s(t)$:

$$\dot{s}(t) = v(t), \quad \dot{v}(t) = a(t), \quad \dot{a}(t) = j(t) \quad (4)$$

The solutions of differential equations have following general form:

$$a(t) = a_0 + j t, \quad v(t) = v_0 + a_0 t + \frac{j}{2} t^2, \quad \Delta s(t) = s_0 + v_0 t + \frac{a_0}{2} t^2 + \frac{j}{6} t^3 \quad (5)$$

In order to apply subsequently eqns (5), we convert them into form of functions:

$$\begin{aligned}a(k, t) &:= a(k, \tau_{k-1}) + j_k t \\ v(k, t) &:= v(k, \tau_{k-1}) + a(k, \tau_{k-1}) t + \frac{j_k}{2} t^2 \\ \Delta s(k, t) &:= v(k, \tau_{k-1}) t + \frac{a(k, \tau_{k-1})}{2} t^2 + \frac{j_k}{6} t^3\end{aligned}\quad (6)$$

In functions (6), we have removed the initial conditions of the displacement equation. The variable $\Delta s(k,t)$ stands for the displacement in each area separately without accumulating it from previous calculations. The index $k=1,2,\dots$ denotes the number of each velocity area, and the value $k=0$ denotes the initial condition before area 1. At any velocity area, we calculate needed parameters assuming initial time $t=0$ and appropriate initial conditions. Following the explanations given in Section 2, we apply eqns (6), for the *case A* when areas 1,2 and 3 exist all together. We predefine:

$$j_0 = 0, \quad j_1 = j_m, \quad j_2 = 0, \quad j_3 = -j_m, \quad \tau_0 = 0, \quad \tau_3 = \tau_1 \quad (7)$$

The indices used in values (7) correspond again to the numbers of velocity areas, and indexing zero stands for initial conditions before area 1.

Although the existence of area 2 requires maximal duration τ_{1m} , we do not use indexing “ m ” intentionally. Replacing maximal values latter, we obtain general solutions avoiding repetitive calculations. Here we apply defined in (6) functions for the first three areas:

In area 1: $t \in [0, \tau_{1m})$, constant positive jerk:

$$\begin{aligned} a(0,0) &= 0, & v(0,0) &= 0, \\ a(1,t) &= j_m t, & v(1,t) &= \frac{j_m t^2}{2}, & \Delta s(1,t) &= \frac{j_m t^3}{6} \end{aligned} \quad (8)$$

In area 2: $t \in [0, \tau_{2m})$, constant positive acceleration:

$$a(2,t) = j_m \tau_1 = \text{const}, \quad v(2,t) = \frac{1}{2} j_m \tau_1 (\tau_1 + 2t), \quad \Delta s(2,t) = \frac{1}{2} j_m \tau_1 (\tau_1 + t) t \quad (9)$$

Even though area 1 exists already, (the acceleration should be maximal), once again, to preserve the generality of the calculations, we assume acceleration at the end of area 1 possibly smaller than a_m .

In area 3: $t \in [0, \tau_{1m})$, constant negative jerk:

$$\Delta s(3,t) = \frac{1}{6} j_m (3\tau_1 (\tau_1 + t) - t^2) t + j_m \tau_1 \tau_2 t \quad (10)$$

All calculations are made in order to obtain needed *switching conditions* between described *cases A,B* and *C*. We need criteria how to classify any required journey. Knowing that in *cases A,B* the acceleration definitely reaches a_m , for area 1, we have following dependencies:

$$\tau_{1m} = \frac{a_m}{j_m}, \quad j_{1m} = \frac{a_m}{\tau_{1m}} \quad (11)$$

In *case A*, the maximal (contract) speed is definitely reached at the end of *area 3*. Using (9) and (11) for the maximal velocity in *area 2* we obtain:

$$v_{2m} = v(2, \tau_{2m}) = \frac{1}{2} a_m (\tau_{1m} + 2\tau_{2m}) \quad (12)$$

On the other hand, v_{2m} is the initial velocity for *area* 3. Following the fact that time slice 3 has duration τ_1 , and observing the symmetry of the increasing/decreasing linear function $a(t)$ in *areas* 1,3, we conclude that the speed in *area* 3 decreases exactly with value v_{1m} , where v_{1m} stands for the maximal speed at the end of *area* 1:

$$v_{1m} = v(1, \tau_{1m}) = \frac{1}{2} j_m \tau_{1m}^2 \quad (13)$$

$$v_{2m} = v_m - v_{1m} = v_m - \frac{1}{2} j_m \tau_{1m}^2 \quad (14)$$

From eqns.(11-14) we derive the maximal duration of time slice τ_1 :

$$\tau_{2m} = \frac{v_m}{a_m} - \tau_{1m} \quad (15)$$

From eqns. (8)-(10) or using directly function (6) we calculate the summary displacement trough *areas* 1,2,3 together with symmetrically equal *areas* 5,6,7. (*Area* 4 is excluded at this point.). The result holds for *cases* A,B,C:

$$s_w = 2(\Delta s(1, \tau_1) + \Delta s(2, \tau_2) + \Delta s(3, \tau_1)) \quad (16)$$

Using simplified result from (16) we define following function:

$$s_w(\tau_1, \tau_2) := j_m \tau_1 (2\tau_1^2 + 3\tau_1 \tau_2 + \tau_2^2) \quad (17)$$

Replacing with appropriate time slices for each *case* A,B,C, (reduced, full, or zeros), as explained in Section 2, and using function (17), we obtain:

Case C, *Non full acceleration, non full velocity*:

The reduced and maximal displacements are

$$s_{C,r} = s_w(\tau_{1r}, 0) = 2 j_m \tau_{1r}^3, \quad s_{C,m} = 2 j_m \tau_{1m}^3 \quad (18)$$

In case when the journey time s_j is smaller than $s_{C,m}$ the tuning slice is $\tau_{1r} < \tau_{1m}$ we solve the equation $s_{C,r} = s_j$ with respect to τ_{1r} and take only the real positive root:

$$\tau_{1r} = \sqrt[3]{\frac{s_j}{2j_m}} \quad (19)$$

Case B, *Full acceleration, non full velocity*:

Again, using function (17), for the case when maximal acceleration is applied, but maximal velocity is not reached (*areas* 2,6), the tuning time slices are $\tau_{2r} < \tau_{2m}$. The displacement is:

$$s_{B,r} = s_w(\tau_{1m}, \tau_{2r}), \text{ or equally} \quad (20)$$

$$s_{B,r} = a_m (2\tau_{1m} + 3\tau_{1m}\tau_{2r} + \tau_{2r}^2)$$

We solve the equation $s_{B,r} = s_j$ with respect to τ_{2r} and we obtain solution

$$\tau_{2r} = \sqrt{\frac{s_j}{a_m^2} + \tau_{1m}^2} - 1.5\tau_{1m} \quad (21)$$

The maximal displacement in *case B*, where $\tau_2 = \tau_{2m}$ is:

$$s_{B,m} = s_w(\tau_{1m}, \tau_{2m}) = \frac{v_m^2}{a_m} + v_m \tau_{1m} \quad (22)$$

Obtained displacements $s_{C,m}$ and $s_{B,m}$ are named *switching displacements*. Comparison with both of them and supposed journey distance s_j is used for immediate recognition of *cases A, B, or C*:

If $s_j \geq s_{B,m}$, then *case A*
 elseif $s_j \geq s_{C,m}$ and $s_j < s_{B,m}$,
 then *case B*
 else *case C*

Case A, Full acceleration and full velocity are reached:

If the journey distance s_j exceeds $s_{B,m}$, the reminding unknown time slice τ_3 (guaranteed to be positive), is found by the equation:

$$\tau_3 = \frac{s_j - s_{B,m}}{v_m}$$

4. Implementation Algorithm for Simultaneous Generation of Velocity Profiles:

We use “ \otimes ” to denote *element by element multiplication* between non-scalar operands. All logical and mathematical operations apply element by element between non-scalar operands or between combination of scalar and non-scalar operands. The annotation “ \neg ” stands for *logical not* over each element of vector. Logical conditions produce digit 1 while the result is “true” and digit 0 while “false”. All bold letter variables represent vectors.

We recollect the dependencies from Subsection 2.2 and Section 3 to suggest a short algorithm generating velocity tables and respective velocity profiles. Presented calculations are extended to implementation in vector form.

Task:

Given maximal allowed jerk j_m , maximal allowed acceleration a_m and maximal velocity v_m . For vector containing n journey distances $s = [s_1, s_2, \dots, s_n]^T$, to calculate respective lookup vectors containing journey time τ_j , s.c.p. parametres ($\tau_{s.c.p.}, s_{s.c.p.}$), and stopping parameters. ($\tau_{stp.}, s_{stp.}$).

Algorithm:

step 1 Calculate scalars related to boundary switching conditions:

$$\tau_{1m} = \frac{a_m}{j_m}, \quad \tau_{2m} = \frac{v_m}{a_m} - \tau_{1m}, \quad s_{C,m} = 2 j_m \tau_{1m}^3, \quad s_{B,m} = \frac{v_m^2}{a_m} + v_m \tau_{1m}$$

step 2 Calculate vectors τ_{1r} and τ_{2r} containing reduced tuning time slices:

$$\tau_{1r} = \sqrt[3]{\frac{\mathbf{s}}{2j_m}}, \quad \tau_{2r} = \sqrt{\frac{\mathbf{s}}{a_m^2} + \tau_{1m}^2} - 1.5 \tau_{1m}$$

step 3 Obtain switching logical vectors needed to switch between cases A, B, C:

$$\mathbf{B} = \begin{cases} 1, & \text{for each } s_j \geq s_{C,m} \text{ and } s_j < s_{B,m}, s_j \in \mathbf{s} \\ 0, & \text{else} \end{cases}$$

$$\mathbf{A} = \begin{cases} 1, & \text{for each } s_j \geq s_{B,m}, s_j \in \mathbf{s} \\ 0, & \text{else} \end{cases}, \quad \mathbf{C} = \neg(\mathbf{A} \vee \mathbf{B})$$

step 4 Calculate time slice vectors τ_1, τ_2, τ_3 , (scalar members related to Fig.1):

$$\tau_1 = \mathbf{C} \tau_{1r} + \neg \mathbf{C} \otimes \tau_{1m}, \quad \tau_2 = \mathbf{A} \tau_{2m} + \mathbf{B} \otimes \tau_{2r}, \quad \tau_3 = \mathbf{A} \otimes \frac{\mathbf{s} - s_{B,m}}{v_m}$$

step 5 Calculate lookup table vectors:

$$\tau_j = 4 \tau_1 + 2 \tau_2 + \tau_3, \quad s_1 = \frac{j_m}{6} \tau_1^3, \quad s_2 = \frac{a_m}{2} \tau_2 \otimes (\tau_2 + \tau_{1m})$$

$$\tau_{s.c.p.} = \neg \mathbf{A} \otimes (\tau_1 + \tau_2) + \mathbf{A} \otimes (\tau_1 + \tau_2 + \tau_3), \quad \tau_{stp} = \tau_j - \tau_{s.c.p.}$$

$$s_{s.c.p.} = s_1 + s_2 + \mathbf{A} \otimes \left(\mathbf{s} - \frac{s_{B,m}}{2} \right), \quad s_{stp} = \mathbf{s} - s_{s.c.p.}$$

END of the algorithm

The time slice vectors obtained in step 4 give sufficient information to draw velocity profiles. Drawing of velocity curves has only illustrative importance. First it is generated time vector \mathbf{t} containing values from 0 to τ_j . Then the jerk $\mathbf{j}(\mathbf{t})$ is segmented into 7 areas (as shown in Fig.1) using unit step function and vectors τ_1, τ_2, τ_3 multiplied by \mathbf{t} . Needed values of $\mathbf{a}(\mathbf{t}), \mathbf{v}(\mathbf{t}), \mathbf{s}(\mathbf{t})$ are obtained from resulting vector $\mathbf{j}(\mathbf{t})$ by subsequent numerical integration with respect to t or using accumulated sums instead of integration.

The results obtained in step 5 are used to create velocity lookup table needed for GC implementation.

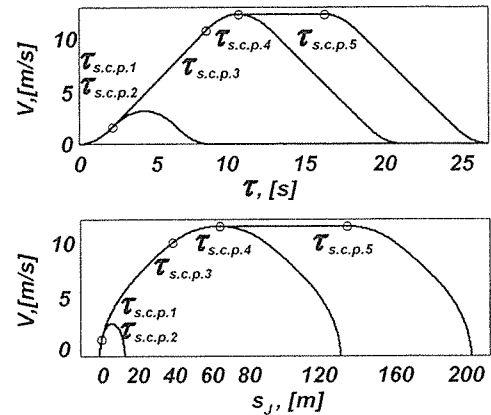
5. IMPLEMENTATION EXAMPLES

Example 1

Referring to the technical reports from web cite of Mitsubishi Electric, the fastest elevator installation in the world, (installed in Landmark Tower Yokohama, Japan), has contract velocity of the elevator cars 750 m/min (12.5 m/s) and max journey distance 267 m. To explore that elevator system, we choose reasonable bounds of a_m and j_m (see Williams et

al. 1985). We choose for illustration $v_m = 12.5 \text{ m/s}$, $a_m = 1.5 \text{ m/s}^2$ and $j_m = 0.7 \text{ m/s}^3$. With presented algorithm we obtain velocity table and draw corresponding curves.

$s, [m]$	$s_{stp}, [m]$	$\tau_{stp}, [s]$	$\tau, [s]$
13.7754	12.6275	6.4286	8.5714
13.7756	13.7756	6.4286	8.5714
130.9523	92.2619	12.6190	20.9524
130.9525	65.4762	10.4762	20.9524
200.0000	65.4762	10.4762	26.4762



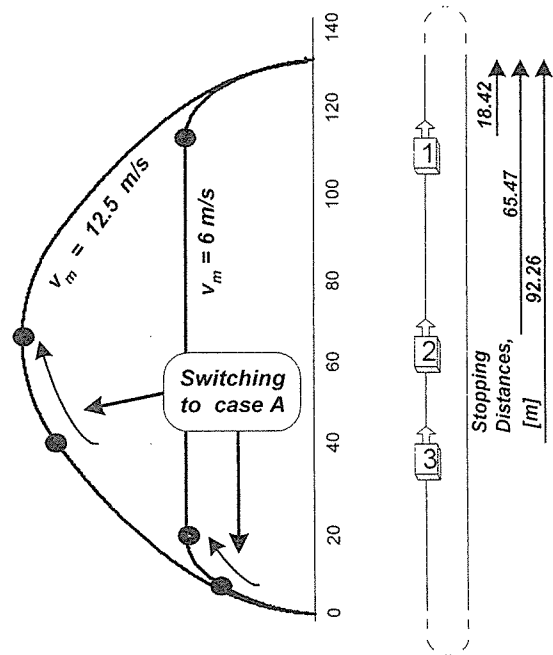
Velocity Table 1, Figure 2, Illustrative velocity curves of Elevator installed in Yokohama building in Japan

Although the 3rd and the 4th velocity curves are overlapping in Fig.2, (rows 3 and 4 in Velocity Table 1), they are differently qualified as being in *cases B* and *A* respectively. The journey distances in rows 3 and 4 of Velocity Table 1 were intentionally chosen to be close to the switching distance $s_{B,m}$. There is a visible jump between the location of 3rd and 4th stop control points. Although the car is increasing its velocity while switching from *case B* to *case A*, the stopping distance is decreasing. Hence, we conclude that comparing with *cases B* and *C*, the car being in *case A* has better ability to stop abruptly.

Example 2

To illustrate how allowed maximal speed affects the journey, in Fig.3 we draw comparison curves between two elevator cars. The parameters of one of the cars, lets call it *car 1* were introduced in Example 1. The second one, *car 2* is assumed to have identical parameters comparing with

car 1, except its lower maximal velocity chosen as 6 m/s. The car with maximal velocity 6 m/s has much smaller stopping distance (18.42 m), while the car with allowed maximal velocity $v_m = 12.5 \text{ m/s}$ has at least 65.5 m stopping distance. However, it is even more important that *car 2* switches much earlier from *case B* to *case A* in comparison with *car 1*. In Example 1 it was already demonstrated that that switching from *case B* to *case A* provokes abrupt decreasing of the stopping distance. We conclude that possibly in heavy traffic conditions, when required stops are too many, the slower car could show better global performance in terms of group control. It has better ability to stop suddenly.



Finally, in Fig. 4 we present family of curves showing the relation between different allowed maximal speeds and stopping parameters. The parameters are obtained from few subsequent velocity tables as the table in Example 1. Obviously, increasing of v_m provokes shortening of expected journey time and losing ability to stop suddenly. We found this problem interesting

for exploration with group control simulator. We expect contradictory effect these two parameters to affect directly waiting time of the passengers. If we define global waiting time of the passengers as a performance criteria, we expect global performance to have a trend shown with dashed line in Fig. 4. Under different traffic circumstances, the maximum is expected to move back and forth. Obtaining of realistic performance curves and their classification is a topic for continuous research using simulator of elevator group control system.

6. CONCLUSION

In this paper, we used a new calculation procedure to generate reference velocity curves for elevator systems. Comparing with similar previous researches, we used shorter methodology avoiding repetitive calculations. Additionally, we considered the minimal journey time focusing on the location of so called stop control point. The stop control point appeared to have jumping nature with significant amplitude. Due to such nonlinear behavior, elevator group control system is shown to be hardly predictable. Also, observing the contradictory effect of stopping distance and the journey time, we concluded that increasing of allowed maximal velocity can decrease global system performance in some cases. We supported our statements by providing implementation algorithm and two examples.

The impact of velocity profiles over global system performance is a subject of further research using simulator of elevator group control.

7. REFERENCES

- Barney G.S. and dos Santos S.M., 1985, *Elevator Traffic Analysis, Design and Control*, UK. Peter Peregrinus Ltd.
- Beldiman, O.V., Wang, H.O., and Bushnell, L.G, 1998, Trajectory generation of high rise/high speed elevators, *American Control Conference*, vol.6, pp. 3455-3459.
- Gagov Z., Cho, Y.C., Kwon W.H., Han B.H., 2000, Timing considerations and kinematics parameters of elevator group control systems, *Elevator Technology 10*, presented in ELEVCON 2000, Berlin, Germany, May 9-11, pp. 245-251.
- Klote, J.H. A method for calculation of elevator evacuation time, 1993, *Journal of Fire Prot. Engr.*, vol. 5, no. 3, pp. 83-95
- Molz H., 1991, On the ideal kinematics of lifts, 1991, *Elevatori*, vol. 1, pp. 41-46
- Peters, R. D., 1995, Ideal lift kinematics: Complete equations for plotting optimum motion, *Elevator Technology, IAEE*, vol. 6, pp. 175-184
- Tanahashi T., Araki H., Drive-control equipment for 750m/min elevators, *Technical Report, MITSUBISHI ELECTRIC*, Japan.
- Williams W.L., McPherson D.G., Mendelsohn A.. 1985, Dynamically generated adaptive elevator velocity profile, *US Patent No. 4,751,984*, owner Otis Elev. Co.
- Yamasaki S., Sugita K., Safety devices for 750m/min elevators, *Technical Report, MITSUBISHI ELECTRIC*, Japan

